Varus malalignment of the lower limb increases the risk of femoral neck fracture: A biomechanical study using a finite element method

D. Belaïd, A. Germaneau, T. Vendeuvre, E. Ben Brahim, K. Aubert, M. Severyns

Version of Record: https://www.sciencedirect.com/science/article/pii/S0020138322002960
Manuscript_4229a85e0e14024c058231d5b4289645

Original research

Varus malalignment of the lower limb increases the risk of femoral neck fracture: a biomechanical study using a finite element method.

D. Belaid (PhD)[1], A. Germaneau (PhD)[2] , T. Vendeuvre (MD, PhD)[2,3],E. Ben Brahim (MD, MSc)[2,3], K. Aubert (PhD) [2], M. Severyns (MD, MSc)[2,4]

[1] *Department of Mechanical Engineering, Faculty of Technology Sciences, University of Mentouri Brothers Constantine P.O Box 325 Ain-El-Bey Way, Constantine, Algeria 25017.*

[2] *Institut Pprime UPR 3346, CNRS – Université de Poitiers – ISAE-ENSMA, France.*

[3]*Department of Orthopaedic Surgery and Traumatology, University Hospital, Poitiers France.*

[4] *Department of Orthopaedic surgery and Traumatology, University Hospital, Martinique, France.*

Corresponding author

Mathieu SEVERYNS, M.D., MSc

Hôpital Pierre Zobda Quitman, 97261 Fort-de-France Cedex, France

Institut Pprime UPR 3346, CNRS – Université de Poitiers – ISAE-ENSMA, France

Email: mathieu.severyns@hotmail.fr

ACKNOWLEDGE

The authors wish to thank Jeffrey Arsham, an American translator, for rereading and correction of the original English-language manuscript.

ABSTRACT.

Introduction: The understanding of the stresses and strains and their dependence on loading direction caused by an axial deformity is very important for understanding the mechanism of femural neck fractures. The hypothesis of this study is that lower limb malalignment is correlated with a substantial stress variation on the upper end of the femur. The purpose of this biomechanical trial using the finite element method is to determine the effect of the loading direction on the proximal femur regarding the malalignment of the lower limb, and also enlighten the relation between the lower limb alignment and the risk of a femoral neck fracture.

Methods: Ten segmentations of CT scans were considered. An axial compression load was applied to the femoral head to digitally simulate the physiological configuration in neutral position as well as in different axial positions in varus/valgus alignment.

Results: **Results**: The stress at the proximal femur changes as the varus _valgus angle does. It can be observed the smaller absolute stress at angle 10^o (valgus) and the higher absolute stress at angle -10° (varus). The mean maximum von Mises stress value was 14.1 (SD=±3.48) MPa for 0^o, while the mean maximum von Mises stress value was 17.96 MPa (SD=4.87) for -10^o in varus. The fracture risk indicator of the proximal femoral epiphyses changes inversely with angle direction. The FRI was the highest at -10° and the lowest at 10°.

Conclusion: Based on the biomechanical findings and the fracture risk indicator determined in this preliminary study, varus malalignment increases the risk of femoral neck fracture. Consideration of other parameters such as bone mineral density and morphological parameters should also help to plan preventive medical strategy in the elderly.

Keywords. Femoral neck fracture – varus malalignment – finite element

Conflict of interests.

All authors declare that they have no conflict of interests for this publication

Funding source

There is no funding source

1 INTRODUCTION

Lower limb alignment is an important consideration in many clinical situations, including fracture reduction, knee arthroplasty and axial correction osteotomy. Malalignment is mainly reported in case of knee osteoarthritis, and it can be both the cause and the consequence. The mechanical axis represents the path of transmission of the load-bearing force relative to the lower extremity. Any deformity in the coronal plane that alters the alignment of the joints of the lower extremity disturbs load-bearing. Although an association between malalignment of the limb segments and knee contact force has been demonstrated [1], very few studies carried out on hip stress distribution due to frontal malalignment [2,3]. On the other hand, some studies have dealt with risk of fracture and direction of loading in relation to the femoral shaft axis in different positions of activity [4]. However, the relationship between the varus or the valgus of the femur mechanical axis or the limb alignment and risk of femoral fracture has not been documented. Understanding stress and strains and their dependence on loading direction caused by an axial deformity could elucidate the mechanism of femur neck fractures [5]. The hypothesis of this study is that lower limb malalignment is correlated with stress variation on the upper femoral area. The objective of this biomechanical work using the finite element method was to determine the effect of the loading direction on the proximal femur caused by the malalignment of the lower limb, and also to clarify the relationship between lower limb alignment and risk of a femoral neck fracture.

2 MATERIALS AND METHODS

This study was conducted at the *Pprime Institut (UPR 3346, CNRS –Poitiers University, France).* To analyze loading distribution and the effect of lower limb alignment, 3D models of the human femur were extracted from medical imaging. Ten intact femurs of ten subjects were imaged in vivo. Data on age and sex, after having removed all personal information as required under the Human Research Ethics protocols, are presented in Table

1. These models are subject to loadings and boundary conditions representing alignment of the lower limb under the effect of varus and valgus deformity.

2.1 Segmentation and meshing

The methodology used to generate the numerical models was to reconstruct the entire femur from the CT scan acquisition. The X-ray scan parameters for the samples were set to 120 kVp, 100 mAs, with 0.75 mm cross-sections and an image matrix of 512 x 512 pixels with a pixel size of 0.434 mm. Volume image segmentation and geometric model were performed using 3D SLICER software (Version 4.11, Kitware, France). The surfaces were then cleaned, healed, closed and filled, the objective being to create two models representing the cortical and the cancellous bones. The finite element models obtained were imported and the analyses were carried out using the ANSYS® WORKBENCH software (Version 2020R2, Ansys Inc, United States) (Figure 1).

Femur bone geometry was discretized using 10-node tetrahedral elements (C3D10) and mesh sensitivity was analyzed versus different element sizes as recommended in the literature [6–8]. The mesh size of models was established following evaluations of convergence in which the variation in estimated stress was less than 1%. Mesh convergence was achieved with elements sized 4 mm in the cortical diaphysis zone; and 2.5 mm in the cortical proximal zone. A refined mesh was then created in the neck zone with a element size equal to 1 mm, the objective being to produce an accurate solution in the fracture region (Figure 1). The cancellous bone was meshed with 4 mm since it had less influence on the global stiffness of the femur. Mesh convergence was achieved with 134506 elements and 226620 nodes for highest-density femur bone, and 106139 elements and 181628 nodes for lowest-density femur.

2.2 Materials

The elastic moduli of the models were assigned to an element-by-element basis assuming heterogeneity and isotropy. For all bone models a Poisson ratio of 0.3 was assumed [9]. Grey scale values were obtained from the CT scan data. The relationship between HU and tissue density was considered linear (equations 1-3) [10]. To produce density–modulus relationships for the whole bone models, several studies have extrapolated the high densities to the low densities and used relationships specific to cortical bone and cancellous bone relationships,

while others have used the intermediate bone densities. In this work the equations calculating Young's modulus of the cortical and cancellous bone were obtained by density-based power law regression (equation 4) [11].

$$\rho_{QCT}(g/cm^3) = 0.007764 \times HU \quad - 0.056148 \tag{1}$$

$$\rho_{ash}(g/cm^3) = 0.877 \times \rho_{QCT} + 0.0789 \tag{2}$$

$$\rho_{app}(g/cm^3) = \rho_{ash}/0.6 \tag{3}$$

$$E(MPa) = 6850 \times \rho_{app}^{1.49} \tag{4}$$

2.3 Alignment axis, load and boundary conditions

To determine the impact of lower extremity alignment on stress magnitude and risk factor, a loading protocol corresponding to a two-legged stance including load bearing through the proximal femoral head was chosen. In this scenario, to simulate the malalignment of the femur it was necessary to designate and identify the mechanical axes or load-bearing axes of the limb and the femur of loading. In relevant studies, alignment of the lower limbs and their main angles have been explored, while some authors have investigated the measurement methods. The whole leg radiograph (WLR), had been used to determine axial alignment in a standing position, or a supine position in 2D [12,13]. In 3D methods, the models reconstructed from CT scan were used to extract the alignment measures and the static mechanical axes [14,15]. The femur mechanical axis (FMA) was regarded as a 3D line connecting femur head center and knee center. The femoral head center was located at the center of the sphere, while the knee center was closed to the mid-diaphyseal point of the femur condyle. Several geometry parameters were measured using the method described in the literature. The neck-shaft angle of the cervico-diaphyseal angle was formed by a line passing through the center of the femoral neck and another line passing through the center of the femoral shaft in the midline [16,17].

In order to measure femur strength, the distal end of the femur was variously constrained. Axial compression load was applied to the femoral head to simulate stance configuration. In the standing positions, inclination of force (F) varied depending on the mal-alignment conditions. During neutral standing position, the joint load vector (F) (in the vertical) was located at an angle of 0° or 3° to the mechanical axis of the lower limb

(automatically the same angle to femoral mechanical axis) [18]. In order to simulate the different misalignments, the reference model was neutral, and the varus and valgus cases were obtained by selecting the rotational center of the femur head and rotating it clockwise or counterclockwise in the coronal plane (or else, the vector force was inclined to the vertical axis). Direction and position of the load were defined as shown in Figure 2. To explore the effect of the malalignment, a load of equal magnitude was applied to all configurations, initiating the fracture by generating stress variations on the femoral upper end or the shaft region.

2.4 Post-processing

Implicit static FE models were analyzed to evaluate femoral constraints and to estimate fracture force. The same loading magnitude was applied to all configurations so as to explore the effect of the malalignment, which was believed to initiate the fracture by generating stress variations in the weak femoral region. In the current study, mechanical analysis was based on visual exploration and stress data extraction. While the von Mises (σ_{vM}) criterion is widely used to predict fracture in finite element biomechanical analyses, it does not consider the difference between compression failure and tensile failure. For this reason, we used the main stress criterion to determine the tensile and compressive strength of the proximal and diaphyseal regions.

Fracture load prediction and failure locations were based on the principal stress criterion or the maximum principal stress failure theory. The fracture of a given element was defined as occurring when maximum stress exceeded the element's ultimate stress. The fracture risk indicator of the proximal femur was used for all load configurations to provide insight into the effects of anatomical variations of the femur, their material properties, and the mechanism of femoral fracture at the neck region. The tensile and compressive fracture risk indicators of the upper end of the femur were the ratio of bone stress to strength stress and can be expressed as:

$$CFRI = FRI = FRI^C = \eta^C = \frac{\sigma^C_{min,ppal}}{\sigma^C_{y,ppl}} \quad (5)$$

$$TFRI = FRI^T = \eta^T = \frac{\sigma^T_{max,ppal}}{\sigma^T_{y,ppl}} \quad (6)$$

For further investigation, fracture propagation was studied. Among the different numerical techniques used to model fracture evolution in the femur, we chose mechanical property degradation through incremental crack

growth [9,19]. To estimate the load fracture and to predict the damage propagation for five femora, a simulated force boundary condition was applied in 50 N increments to the femoral head surface. After each load step, elements with the principal stress σ_{ppl}() exceeding the yield stress ($\sigma_{Y,ppl}$) were "failed" by assigning a very small Young's modulus (1 MPa). The relationships between $\sigma_{y,ppl}$t and ρ_{app} proposed by Kheirollahi et al [20] were stated as:

$$\sigma_y = 116\rho_{ash}^{2.03}(MPa) \qquad (7)$$

Model stiffness was then updated, the load was increased, and the model was solved again until the QCT/FEA load/displacement curve reached a plateau.

3 RESULTS

Alignment of lower limb influences stress distribution in the upper end of the femur was produced under the two leg standing position. Misalignment-caused deformity influences risk of fracture, load failure value and the fracture location.

3.1 Stress distribution

The first results indicate that stresses vary according to the angle of femur inclination in relation to the load-bearing axis. Figure 3 describes the variation of peak von Mises stress. The curves show a decrease in stress by increasing the valgus angle with respect to the neutral position. Stress increase through increased varus angle in a neutral position is very remarkable. The mean maximum von Mises stress value was 14.1 (SD=±3.48) MPa for 0^o, while the mean maximum von Mises stress value was 17.96 MPa (SD=4.87) for -10^o in varus deformity (Table 2).

Figure 4 represents the varus-valgus configuration at -10^o, -5^o, 5^o, 10^o and at the neutral position 0^o of a subject taken as an example. In all configurations the upper end of the femur and the superior and inferior surfaces of the femoral neck experience tensile and compressive stresses. Under the same load but with different angle

direction, overall maximum principal stress was localized at the same superior cortex of the femoral neck in all the models, while the minimum principal stress was localized at the same inferior cortex of the femoral neck.

Stress at the proximal part of the femur was modified by changing the varus -valgus angle. The lowest absolute stress was found at 10^{o} and the highest abs at -10^{o}. Mean maximum principal stress at the proximal femur stress was 12.56 MPa (SD=±4.14) for -10^{o} (varus), and decreased to 9.44 MPa (SD=±3.24) for 0^{o} and to 6.48 MPa (SD=±2.49) for +10°. In addition, absolute mean minimum principal stress at the proximal femur was 17.11 (SD=±4.59) for -10°, and decreased to 15.11 MPa (SD=±4.08) for 0^{o} and to 12.69 MPa (SD=±3.5) for 10^{o} (table 3).

3.2 Fracture Risk at all inclination angles

To investigate the effect of malalignment on risk of femoral neck fracture risk, fracture indicators and tensile and compressive strengths for the proximal femur were calculated separately. The distribution of the compressive fracture risk indicator $\boldsymbol{FRI_P^C}$ and the tensile fracture indicator $\boldsymbol{FRI_P^T}$ at the superior and inferior aspects (and vice versa) of the proximal femur was shown and compared in Figure 5 for the two leg-stance configurations.

Mean $\boldsymbol{FRI_P^C}$ at the proximal femur ranged from 0.193 (SD= ± 0.097) to 0.125 (SD=±0.058) at the inferior area, and the mean $\boldsymbol{FRI_P^T}$ ranged from 0.198 (SD=±0.059) to 0.104 (SD=±0.042) at the superior area, which is often a sign of hip fracture in the elderly. The Fracture risk indicator of the proximal femoral epiphyses changes inversely with angle direction; it was highest at -10° (varus) and lowest at 10° (valgus) (Table 4).

3.3 Fracture load and fracture location

Another set of results was obtained from linear analyses. Average nodal displacements of all the nodes for the femoral head in each step were calculated and load-displacement diagrams were obtained for each subject. The FE model accurately estimated the fracture load in all subjects under the two-leg stance-loading configuration, while the fracture site and pattern were localized according to the valgus/varus configuration.

Figure 6 shows the finite element analyses (FEA) load-displacement curve results for a specimen as an example. The maximum load in these diagrams was considered as ultimate femoral strength. The 3D FE analysis found the distribution of displacements within the femur and the failure forces of all subjects at neutral position. The yield point was estimated at 2880 (SD=±824.31) N and failure load was 3500 (SD=±735.69). Load failure varied substantially between the ten subjects when the loading conditions for the patients' anatomically alignment were the same (neutral position). The fracture appeared in the femoral neck in all models. The two largest results were change load failure when changing the load direction angle and the location of the fracture. The variation of varus/valgus malalignment resulted in modified femoral load failure. Increasing valgus generally led to increased hip load failure, whilst increasing varus malalignment generally resulted in decreased load failure at the proximal femur.

4 DISCUSSION

The study shows that malalignment or loading conditions caused by malalignment can change the transfer load by means of a relatively simple FE model including individual material properties of the bone. In fact, the subject-specific FE model predicted the fracture load. Numerical results showed the influence of alignment deformities and the initial crack path varied with different inclination angles of the femora. The prediction of patient-specific femur mechanical response to various load conditions is of major clinical importance in orthopedics. Restoration of a neutral mechanical axis improves implant durability and patient function following surgery. Almost all published studies have focused on simulation of a single loading condition, mimicking either the stance phase of gait or an unprotected fall to the side. Therefore, it is necessary to investigate the influence of misalignment. In our investigation, CT-based FE models were created to analyze the transfer of load and to evaluate femur fracture risk, the objective to estimate femoral fracture load type in a two-leg stance condition in varus and valgus load configuration.

4.1 Femoral stress in neutral configuration

Several aspects of stress magnitude and distribution for the cases examined are worth highlighting. Biomechanical stress analyses were conducted to investigate the effects of lower limb alignment factors on relative femur stress distribution. Firstly, stress distribution in the neutral position with the mechanical axis of the femur had the same trajectory of the load axis (angle $=0^{o}$) and showed peak von Mises stress aim the upper end of the femur. In the common anatomy, stress concentration occurred at the inferior root of the femoral neck in the compressive stress mode; while stress concentration occurred at the superior root of the femoral neck ins the tensile stress mode. The location of the stress patterns produced in these models was very similar to that obtained in earlier vertical loading studies [21,22]. In each stance, the stress pattern indicated that the superior aspect of the neck and the anterolateral aspect of the shaft were under tension.

Moreover, regarding location of the fracture in the neutral position, all models were fractured at the neck, which was illustrated by the risk facture indicator and confirmed by the pattern fracture using the principal stress criterion. Several works have loaded the femur, taking into account the axis of the femoral diaphysis to simulate proximal fracture, and other investigations have used the mechanical axis of femur as a reference of the loading presentation. To compare our results, we had to consider the anatomy, geometry and parameters considered to design the load axis of the femur. For example, the angle between the mechanical axis and the anatomical axis of the femur is usually 7 ±2° [15] and the mechanical axis of the lower extremity corresponds to an approximately 3° slope compared with the vertical axis [23,24].

In current FE analysis, the ultimate force fracturing the femur was taken as the peak value for the curve. The average ultimate numeric force in neutral position was 2880 ± 824.31 N (range: 2200– 4150 N) for two-limb stance configurations. These findings are consistent with those reported in the literature. Indeed, prior investigations of uniaxial quasi-static compression analysis performed on 55 femurs conducted by Falcinelli et al [25], loaded at 0° in the coronal plane, yielded failure loads in the range of 1299 - 10,024 N. Bessho et al [26] found under identical conditions (mechanical axis load) a range of 1875- 3375 N for patients with hip fracture and a range of 4375 -5875 N for healthy volunteers.

4.2 Correlation between Femoral Neck Fracture and valgus/varus configurations.

The FE femur models under a valgus or varus load condition were compared to t neutral load condition during a two-leg stance configuration. Relative to the neutral position, both valgus and varus configurations increased peak von Mises stress.

Regarding the proximal femur, the highest stress was met at -10° and decreased gradually by increasing the angle direction. The change in load direction increases stresses in some regions and reduces them in others. If these changes are large, they can lead to adaptive bone remodeling. Filardi at al [27], investigated the stress shielding and its influence on the integrity and resistance of bones in the presence of 4^{o} varus or valgus positioning of the knee in long chain leg. Equivalent von Mises stress results revealed two significant peaks on the hip of the femur in the valgus and varus configurations. Mean von Mises stress at neutral position, in this study was 0.28 times higher than our results. However, various studies have confirmed the influence of load condition and boundary condition in femur stress response. The FE study of Faisal and Luo [20] indicated two critical regions. In single weight bearing the highest peak stresses was located at the middle shaft region and the second was located at the neck, showing that the half femur model exhibited higher stress than the whole femur model.

In this study, the response of the whole femur taking its mechanical axis as the reference was highlighted. The results showed the regular course of stress in the shaft in the neutral loading cases, warranting the conclusion that the load situation in question closely resembles that of pure bending. In load situations of both the extreme varus and valgus, the maximum value of the stress in longitudinal direction doesn't occur in the neck but in the part of the shaft on the medial side in valgus load and in the distal antero-lateral in varus load. Overall, the high stress magnitude indicates the critical region to fracture. The fracture indicator risk used in this investigation clarified the critical region to fracture under stance configuration and the influence of the varus or valgus load directions. Regarding FRI for the upper end of the femur, we observed a linear trend decreasing from the varus to the valgus. Compared to the neutral load, the compressive and the tensile FRI of proximal femur showed that the varus load increased risk of fracture at the neck, which decreased load failure whereas the valgus load decreased the risk of fracture at the neck, which increased load failure.

To identify the loading conditions under which the femur is most likely to fracture and to prevent hip fracture, most studies have analyzed the effects of load conditions of the hip femur. They have considered two loads configurations, at stance and at sideways fall. Kheirollah et al [20], used strain energy FRI and loaded the

femur head in the direction of the shaft, and Faisal et al [21], used FRI while considering the maximum principal stresses criterion generated at the femoral neck area, as well as corresponding tensile and compressive yield strengths, and observed that the femoral neck more clearly explains the severity of sideways fall than single-stance load. In the stance configuration, various load direction were used to predict femur failure according to daily activity loads such as: slow walking, normal walking, fast walking, upstairs, downstairs, standing up, sitting down, standing on 2-1-2 legs. Bending of the knee can vary the inclination of the resultant hip force on the head of the femur. Other authors have studied the potential for low- and high-load physical activities that has been suggested to offset the detrimental effect of osteoporosis and to assess the risk for femoral neck fractures during such activities. Their results enhance that activities involving maximum hip-extension and knee-flexion contractions are possible alternatives to high-impact activities (e.g., one-legged long jump) to promote femoral neck bone formation [28]. The effect of load direction at the stance configuration on fracture load and on hip fracture risk were examined by Keyak and al [29]. Using CT scan-based linear FE models of the proximal femur, quantified the effect of force direction on fracture load, a factor inherently associated with fracture risk. They found that at the small posterior component, the lowest fracture loads for the force directions occurred when the lateral component was small. These findings are further supported by the results of our FE model predictions, in which the femoral hip is most likely to fracture in high magnitude valgus loading conditions.

The femur has a complex anatomic geometry, which varies depending on human body anatomy. The geometric parameters such as cervical-diaphyseal angle, angle between diaphyseal axis and mechanical axis vary in the healthy adult. These parameters influence the response of the femur. Some studies [10,30,31] investigated the biomechanical effects of individual geometric parameters in the femoral neck as independent variables through computational modeling and simulation using virtual bones (computer models). Their results suggest that a smaller neck-shaft angle and a longer neck are significant risk factors for stress fractures of the femoral neck, particularly for the unstable type of tension fracture that starts s at the superior cortex. In an unscathed femur, high compressive stresses were mostly produced in the femoral neck. Qian et al [32] examined five different sites around the hip joint in healthy and fractured femurs. Their investigation showed that bone mineral density (BMD) for the patients who suffered from a femoral-neck fracture was significantly smaller in all examined areas around femoral neck. Under a similar loading of usual standing condition but with different femoral-neck–shaft angle using a finite element model and computer simulation, results showed that maximum stress in the femoral-neck region is inversely related to the femoral-neck angle, which corresponds to our

findings. Our results, in the neutral position configuration, have shown that both femoral neck length and neck-shaft angle affect the biomechanical risk of femoral neck stress fracture. A smaller femoral neck-shaft angle can not only increase the risk for femoral neck stress fracture, but is also a key risk factor for the unstable tension type of fracture. Moreover, femur length effects the load failure, while high length increases the failure force [33].

4.3 Limitations

The main limitation of the present study was the availability of only five human femurs, a factor that prevented the evaluation of geometric parameters. Furthermore, there was no availability of cohort specimens to extract information about the BP for additional study. In addition the study may have introduced certain biases into the results such as the correlation between the BMD, geometry and alignment. In addition, interpretation was limited due to the small number of subjects. It was clarified whether subjects with abnormal alignment have different femoral neck fracture locations. To confirm this hypothesis, prospective cohort studies including investigations of lower limb alignment, geometrical parameters and BMD distribution as well as the occurrence of atypical femoral fractures (AFF) in adequately sized populations are required. Research regarding femoral-neck fractures has mainly focused on bone mineral density [34,35] and it is important to remember that anatomy and bone quality are unique to each specimen.

This study provides quantitative information regarding the femoral mechanical axis factor that influence strength of the proximal femur on elderly subjects. These findings provide insight into the evaluation of hip fracture risk and were completed with fracture localization investigation. They highlighted that biomechanical factors, such as femoral bone geometry and lower limb alignment, are related to the location where the mechanical stresses are concentrated. Therefore, malalignment in the lower limbs associated with bone tissue properties would be one of the risk factors for the accumulation of the micro-cracks in the lateral cortex and progression to AFF. Geometrical factors related to the femur and lower limb alignment are related to the concentration of mechanical force. Physicians should recognize the risk factors for the development of AFF, as well as signs of AFF, the objective being to provide adequate treatment for patients. More research will provide better evidence related on these topics and contribute to establish evidence-based treatment for AFF. The

clinical potential of a biomechanical investigation is to assess fracture risk and prevention strategies such as more targeted drug treatment for a better trabecular quality in osteoporosis.

5 CONCLUSION

In conclusion, the results of this study demonstrate a clear dependence of the individual axial alignment on stress distribution to the upper end of the femur. Based on the biomechanical findings and the fracture risk indicator determined in this preliminary study, varus malalignment increases the risk of femoral neck fracture. The inclusion of other parameters such as bone mineral density and morphological parameters should also help in planning preventive medical strategy in the elderly.

6 CONFLICT OF INTEREST

All the authors declare they have no conflict of interest.

7 FUNDING

No funding sources.

8 REFERENCES

[1] Holden null, Stanhope null. The effect of variation in knee center location estimates on net knee joint moments. Gait Posture 1998;7:1–6. https://doi.org/10.1016/s0966-6362(97)00026-x.

[2] Eckstein F, Hudelmaier M, Cahue S, Marshall M, Sharma L. Medial-to-lateral ratio of tibiofemoral subchondral bone area is adapted to alignment and mechanical load. Calcif Tissue Int 2009;84:186–94. https://doi.org/10.1007/s00223-008-9208-4.

[3] Lerner ZF, DeMers MS, Delp SL, Browning RC. How tibiofemoral alignment and contact locations affect predictions of medial and lateral tibiofemoral contact forces. J Biomech 2015;48:644–50. https://doi.org/10.1016/j.jbiomech.2014.12.049.
[4] Khoo BCC, Brown K, Cann C, Zhu K, Henzell S, Low V, et al. Comparison of QCT-derived and DXA-derived areal bone mineral density and T scores. Osteoporos Int 2009;20:1539–45. https://doi.org/10.1007/s00198-008-0820-y.
[5] Yoganandan N, Banerjee A, Hsu F-C, Bass CR, Voo L, Pintar FA, et al. Deriving injury risk curves using survival analysis from biomechanical experiments. J Biomech 2016;49:3260–7.

https://doi.org/10.1016/j.jbiomech.2016.08.002.
[6] Grassi L, Väänänen SP, Ristinmaa M, Jurvelin JS, Isaksson H. How accurately can subject-specific finite element models predict strains and strength of human femora? Investigation using full-field measurements. J Biomech 2016;49:802–6. https://doi.org/10.1016/j.jbiomech.2016.02.032.
[7] Ali AA, Cristofolini L, Schileo E, Hu H, Taddei F, Kim RH, et al. Specimen-specific modeling of hip fracture pattern and repair. J Biomech 2014;47:536–43. https://doi.org/10.1016/j.jbiomech.2013.10.033.
[8] Haider IT, Goldak J, Frei H. Femoral fracture load and fracture pattern is accurately predicted using a gradient-enhanced quasi-brittle finite element model. Med Eng Phys 2018;55:1–8. https://doi.org/10.1016/j.medengphy.2018.02.008.
[9] Hambli R, Allaoui S. A robust 3D finite element simulation of human proximal femur progressive fracture under stance load with experimental validation. Ann Biomed Eng 2013;41:2515–27. https://doi.org/10.1007/s10439-013-0864-9.
[10] Schileo E, Dall'ara E, Taddei F, Malandrino A, Schotkamp T, Baleani M, et al. An accurate estimation of bone density improves the accuracy of subject-specific finite element models. J Biomech 2008;41:2483–91. https://doi.org/10.1016/j.jbiomech.2008.05.017.
[11] Morgan EF, Bayraktar HH, Keaveny TM. Trabecular bone modulus-density relationships depend on anatomic site. J Biomech 2003;36:897–904. https://doi.org/10.1016/s0021-9290(03)00071-x.
[12] Nguyen A-D, Shultz SJ. Sex differences in clinical measures of lower extremity alignment. J Orthop Sports Phys Ther 2007;37:389–98. https://doi.org/10.2519/jospt.2007.2487.
[13] Brouwer RW, Jakma TSC, Bierma-Zeinstra SMA, Ginai AZ, Verhaar JAN. The whole leg radiograph: standing versus supine for determining axial alignment. Acta Orthop Scand 2003;74:565–8. https://doi.org/10.1080/00016470310017965.
[14] Hirschmann MT, Hess S, Behrend H, Amsler F, Leclercq V, Moser LB. Phenotyping of hip-knee-ankle angle in young non-osteoarthritic knees provides better understanding of native alignment variability. Knee Surg Sports Traumatol Arthrosc 2019;27:1378–84. https://doi.org/10.1007/s00167-019-05507-1.
[15] Subburaj K, Ravi B, Agarwal M. Computer-aided methods for assessing lower limb deformities in orthopaedic surgery planning. Comput Med Imaging Graph 2010;34:277–88. https://doi.org/10.1016/j.compmedimag.2009.11.003.
[16] Hagen JE, Miller AN, Ott SM, Gardner M, Morshed S, Jeray K, et al. Association of atypical femoral fractures with bisphosphonate use by patients with varus hip geometry. J Bone Joint Surg Am 2014;96:1905–9. https://doi.org/10.2106/JBJS.N.00075.
[17] Oh Y, Fujita K, Wakabayashi Y, Kurosa Y, Okawa A. Location of atypical femoral fracture can be determined by tensile stress distribution influenced by femoral bowing and neck-shaft angle: a CT-based nonlinear finite element analysis model for the assessment of femoral shaft loading stress. Injury 2017;48:2736–43. https://doi.org/10.1016/j.injury.2017.09.023.
[18] Paley D, Pfeil J. [Principles of deformity correction around the knee]. Orthopade 2000;29:18–38. https://doi.org/10.1007/s001320050004.
[19] Marco M, Giner E, Caeiro-Rey JR, Miguélez MH, Larraínzar-Garijo R. Numerical modelling of hip fracture patterns in human femur. Comput Methods Programs Biomed 2019;173:67–75. https://doi.org/10.1016/j.cmpb.2019.03.010.

[20] Kheirollahi H, Luo Y. Assessment of Hip Fracture Risk Using Cross-Section Strain Energy Determined by QCT-Based Finite Element Modeling. Biomed Res Int 2015;2015:413839. https://doi.org/10.1155/2015/413839.
[21] Faisal TR, Luo Y. Study of stress variations in single-stance and sideways fall using image-based finite element analysis. Biomed Mater Eng 2016;27:1–14. https://doi.org/10.3233/BME-161563.
[22] Cristofolini L, Juszczyk M, Martelli S, Taddei F, Viceconti M. In vitro replication of spontaneous fractures of the proximal human femur. J Biomech 2007;40:2837–45. https://doi.org/10.1016/j.jbiomech.2007.03.015.
[23] Cherian JJ, Kapadia BH, Banerjee S, Jauregui JJ, Issa K, Mont MA. Mechanical, Anatomical, and Kinematic Axis in TKA: Concepts and Practical Applications. Curr Rev Musculoskelet Med 2014;7:89–95. https://doi.org/10.1007/s12178-014-9218-y.
[24] Luo C-F. Reference axes for reconstruction of the knee. Knee 2004;11:251–7. https://doi.org/10.1016/j.knee.2004.03.003.
[25] Falcinelli C, Schileo E, Balistreri L, Baruffaldi F, Bordini B, Viceconti M, et al. Multiple loading conditions analysis can improve the association between finite element bone strength estimates and proximal femur fractures: a preliminary study in elderly women. Bone 2014;67:71–80. https://doi.org/10.1016/j.bone.2014.06.038.
[26] Bessho M, Ohnishi I, Okazaki H, Sato W, Kominami H, Matsunaga S, et al. Prediction of the strength and fracture location of the femoral neck by CT-based finite-element method: a preliminary study on patients with hip fracture. J Orthop Sci 2004;9:545–50. https://doi.org/10.1007/s00776-004-0824-1.
[27] Filardi V. Stress shielding in the bony chain of leg in presence of varus or valgus knee. J Orthop 2015;12:102–10. https://doi.org/10.1016/j.jor.2014.06.007.
[28] Martelli S, Kersh ME, Schache AG, Pandy MG. Strain energy in the femoral neck during exercise. J Biomech 2014;47:1784–91. https://doi.org/10.1016/j.jbiomech.2014.03.036.
[29] Keyak JH, Skinner HB, Fleming JA. Effect of force direction on femoral fracture load for two types of loading conditions. J Orthop Res 2001;19:539–44. https://doi.org/10.1016/S0736-0266(00)00046-2.
[30] Lotz JC, Cheal EJ, Hayes WC. Fracture prediction for the proximal femur using finite element models: Part I--Linear analysis. J Biomech Eng 1991;113:353–60. https://doi.org/10.1115/1.2895412.
[31] Panyasantisuk J, Pahr DH, Zysset PK. Effect of boundary conditions on yield properties of human femoral trabecular bone. Biomech Model Mechanobiol 2016;15:1043–53. https://doi.org/10.1007/s10237-015-0741-6.
[32] Qian J-G, Song Y-W, Tang X, Zhang S. Examination of femoral-neck structure using finite element model and bone mineral density using dual-energy X-ray absorptiometry. Clin Biomech (Bristol, Avon) 2009;24:47–52. https://doi.org/10.1016/j.clinbiomech.2008.09.007.
[33] Holzer G, von Skrbensky G, Holzer LA, Pichl W. Hip fractures and the contribution of cortical versus trabecular bone to femoral neck strength. J Bone Miner Res 2009;24:468–74. https://doi.org/10.1359/jbmr.081108.
[34] Gong H, Zhang M, Fan Y, Kwok WL, Leung PC. Relationships between femoral strength evaluated by nonlinear finite element analysis and BMD, material distribution and geometric morphology. Ann Biomed Eng 2012;40:1575–85. https://doi.org/10.1007/s10439-012-0514-7.
[35] Kanis JA, McCloskey EV, Johansson H, Oden A, Melton LJ, Khaltaev N. A reference standard for the description of osteoporosis. Bone 2008;42:467–75. https://doi.org/10.1016/j.bone.2007.11.001.

9 FIGURES

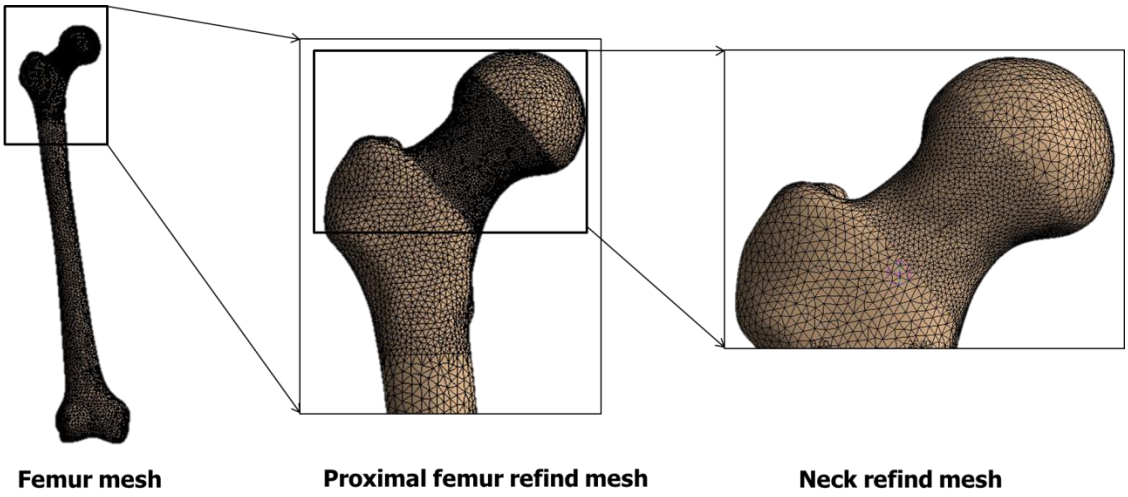

Figure 1. Femur meshes and refines areas.

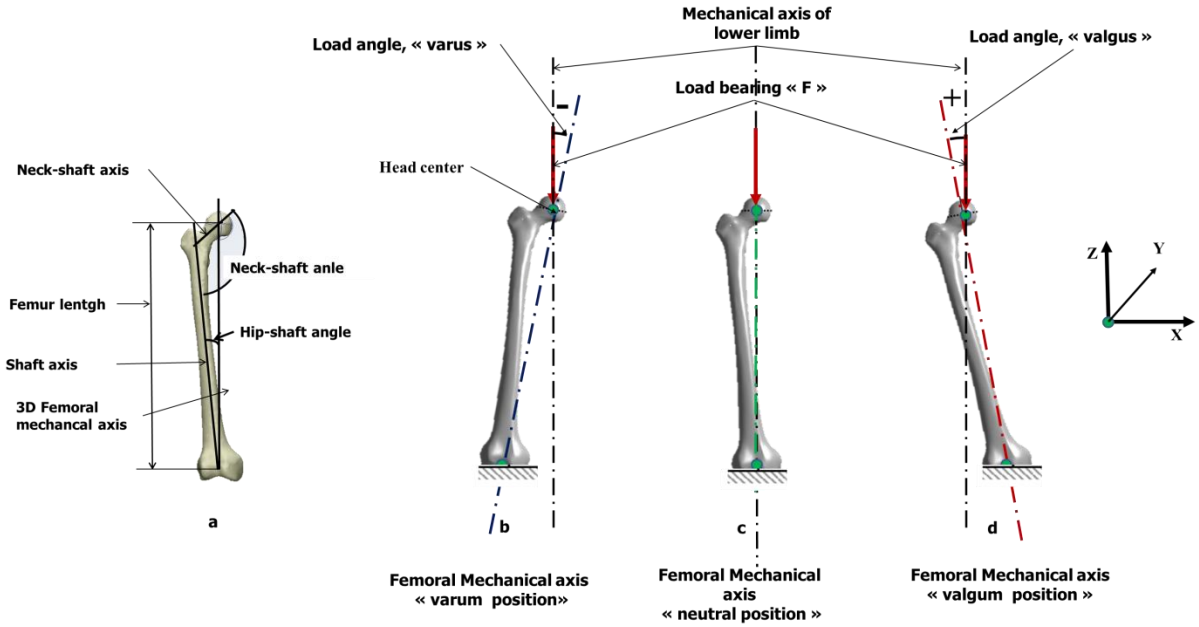

Figure 2. a) Geometrical parameters. Alignment and boundary conditions applied on the femur. b) Varus position with a negative angle, c) In neutral position, the limb is vertical (angle 0°), d) Valgus position with a positive angle.

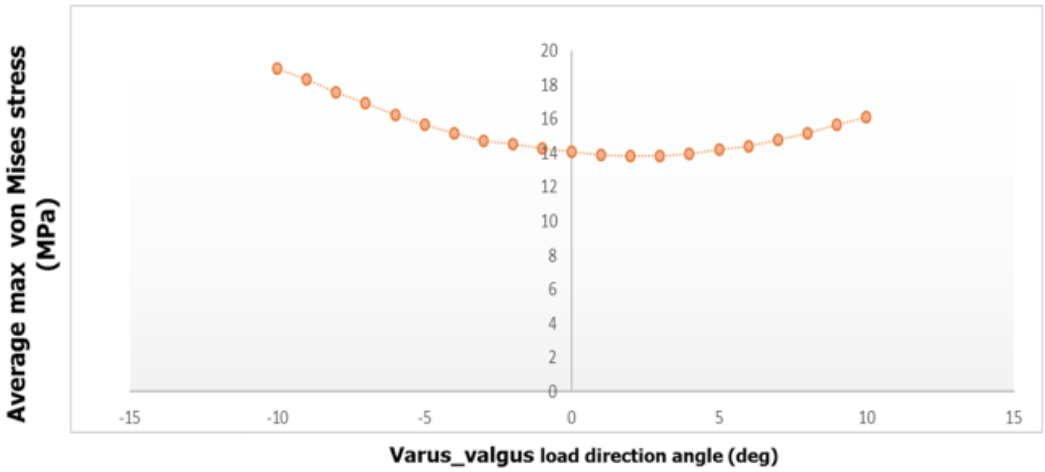

Figure 3. Maximum von Mises stress according to the varus/valgus angle

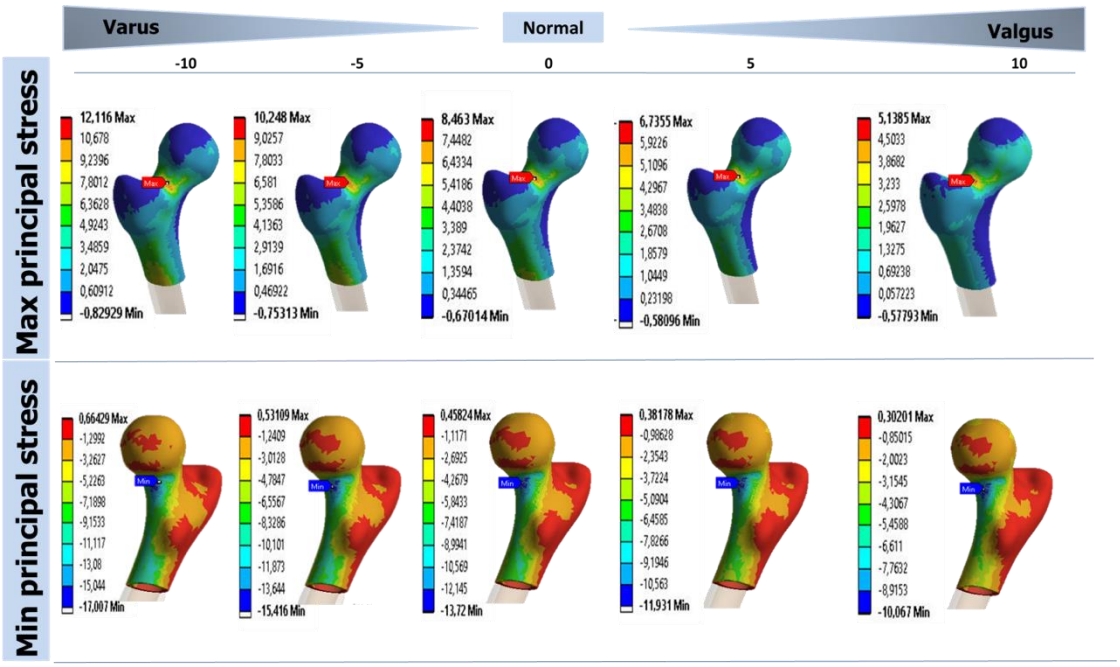

Figure 4. Example of Principal stress distribution (MPa) on the upper end of the femur

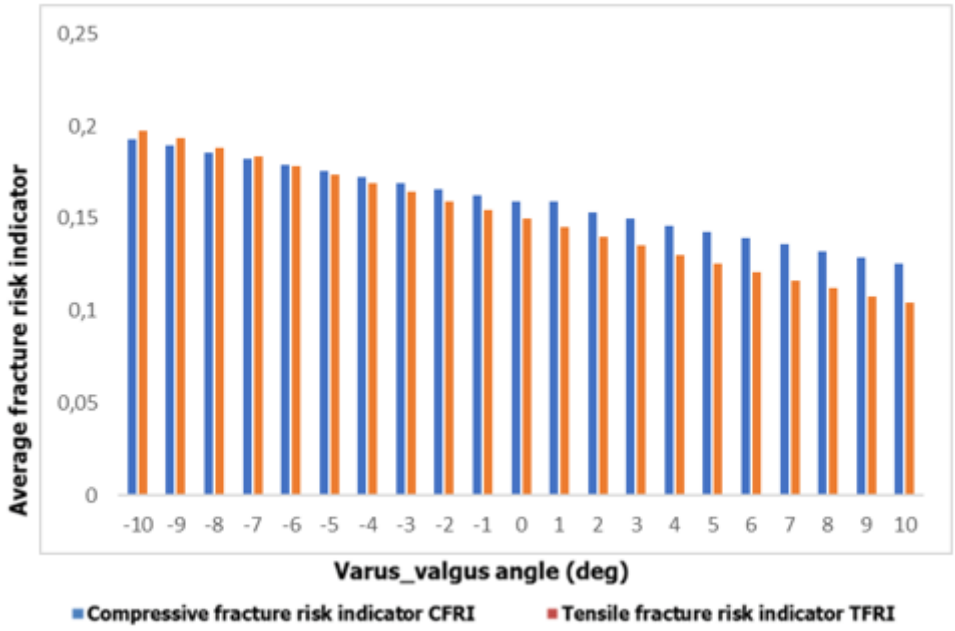

Figure 5. Risk fracture indicators of the femoral neck area at all the configurations of varus/valgus deformation.

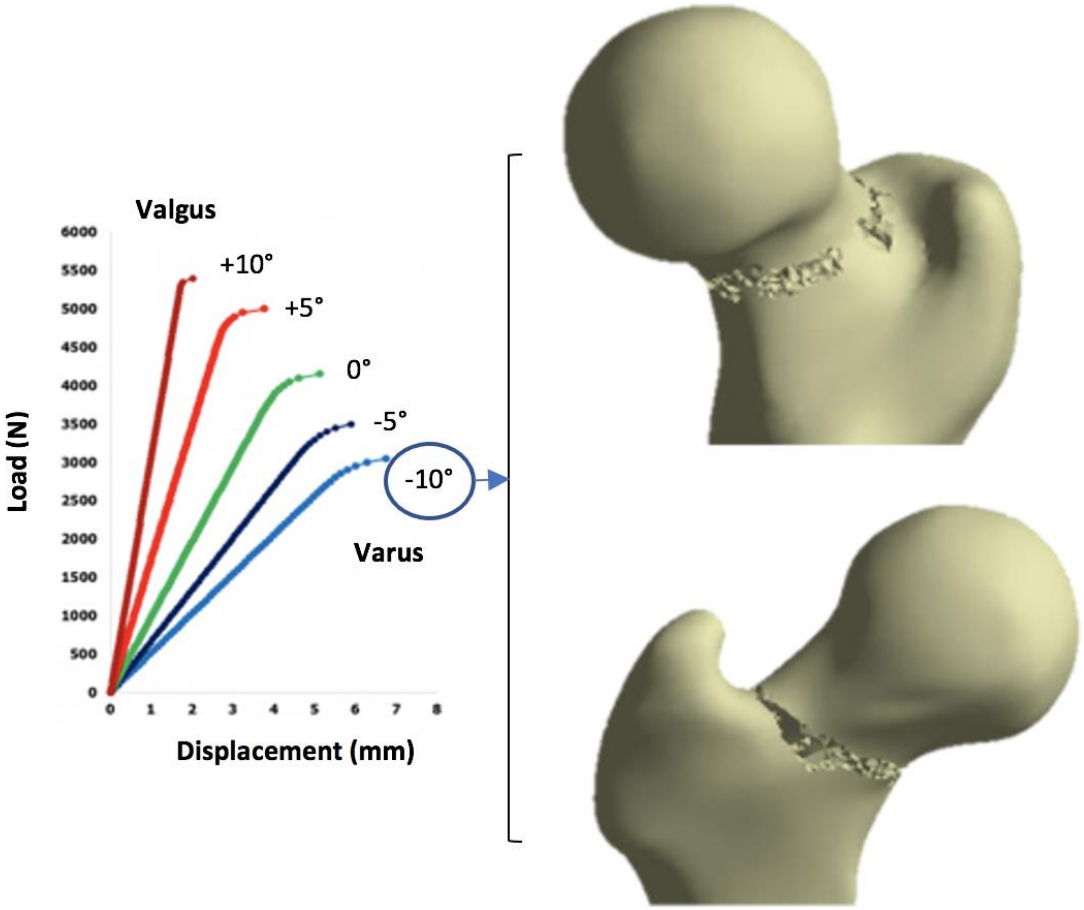

Figure 6. Fracture site and force displacement curves at different load angles: -10°, -5°, 0°, 5°, 10°, and FE view at 10° of varus malalignment.